



SEISMIC ASSESSMENT OF SCHOOL BUILDINGS IN ITALY: RETROFIT AND RISK CLASSIFICATION

W. Carofilis ⁽¹⁾, D. Perrone ⁽²⁾, G. O'Reilly ⁽³⁾, R. Monteiro ⁽⁴⁾, A. Filiatrault ⁽⁵⁾, ⁽⁶⁾

⁽¹⁾ Research fellow, University School for Advanced Studies IUSS Pavia, wilson.carofilis@iusspavia.it

⁽²⁾ Postdoctoral researcher, University School for Advanced Studies IUSS Pavia, daniele.perrone@iusspavia.it

⁽³⁾ Assistant Professor, University School for Advanced Studies IUSS Pavia, gerard.oreilly@iusspavia.it

⁽⁴⁾ Associate Professor, University School for Advanced Studies IUSS Pavia, ricardo.monteiro@iusspavia.it

⁽⁵⁾ Professor, University School for Advanced Studies IUSS Pavia, andre.filiatrault@iusspavia.it

⁽⁶⁾ Professor, State University of New York at Buffalo, af36@buffalo.edu

Abstract

The potentially high vulnerability and poor performance of existing school buildings in Italy, reported after past seismic events, has raised awareness of the need to improve their seismic performance. In this context, a research project dealing with assessing the seismic risk of school buildings was conducted on representative typologies of the school building population in Italy. This paper explores some retrofit strategies for three specific school buildings representing the most common typologies of the Italian school building stock. A performance assessment was carried out using detailed numerical models developed to recreate the main structural deficiencies documented in similar buildings. Based on the performance assessment, retrofit schemes were proposed to address the main structural deficiencies and to meet code requirements for the different limit states. These requirements are set to limit the damage to non-structural elements and prevent non-ductile failure mechanisms in the structural systems, following a typical code and practitioner-oriented process. The retrofit alternatives were then evaluated through increasing shaking intensities to quantify risk-based decision variables such as expected annual loss and collapse safety. The results indicate the efficiency of the retrofit options utilized in reducing both the economic losses and collapse vulnerability of the buildings. Finally, the seismic risk classification guidelines, implemented recently in Italy, were applied at a national scale to estimate the seismic risk on existing school buildings in the Italian peninsula and the risk reduction achieved by each retrofit alternative. Consequently, budget programs can be derived based on national risk maps, prioritizing the investment of seismic retrofit interventions in regions of vulnerable school buildings.

Keywords: performance assessment, failure mechanism, retrofit, loss estimation.



1. Introduction

The importance of the seismic vulnerability assessment of critical facilities, such as school buildings, has been pointed out by many research studies in recent years. A research project carried out at the European Centre for Training and Research in Earthquake Engineering (EUCENTRE) investigated the seismic vulnerability of typical Italian school buildings. From the database collected by Borzi *et al.* [1], it was found that 80% of school buildings in Italy comprise both unreinforced masonry (URM) and reinforced concrete frames with masonry infill (RC), whereas the remaining 20% are characterized by other typologies, such as precast structures (PC), steel constructions or mixed assemblies [2]. The damage observed during past seismic events [3, 4] pointed out that the RC, PC and URM typologies represent the most vulnerable structures and therefore they were selected as representative case study school buildings for this study.

The case study school buildings are located in different regions of Italy. Schematic views of the three buildings are displayed in Fig. 1. The RC school building has three stories, while the PC and URM buildings consist of two stories. The three school buildings were constructed in the 1960s, 1980s and 1990s, respectively. The model of the RC school building was developed with the OpenSees software [5]. Likewise, the PC school building model was created in OpenSees. The URM school building, on the other hand, was modelled in the TreMuri software [6]. Further details on the main features and numerical modelling of these school buildings can be found in O'Reilly *et al.* [7].

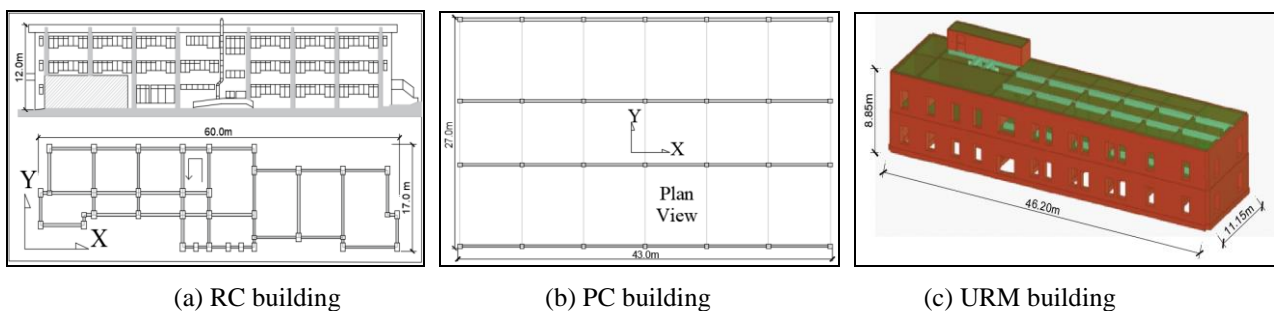


Fig. 1 - Case study school building configurations

The structural performance of the school buildings was evaluated through the N2 method, using the guidelines by Fajfar [8] and Dolšek and Fajfar [9, 10] (for RC frames with infills walls). Therefore, the uniform hazard spectra (UHS) were calculated at different return periods for the city of Cassino, Italy - the actual location of one of the school buildings. According to the prescriptions of NTC 2018 [11], four different return periods were selected: 45, 75, 712 and 1463 years, corresponding respectively, to: SLO: operational limit state; SLD: damage limitation limit state; SLV: life safety limit state; and SLC: collapse prevention limit state, for a building class III with a nominal service life of 75 years [11] (i.e. school buildings). Additionally, a multiple-stripe analysis (MSA) was conducted along with a probabilistic seismic hazard analysis (PSHA). The hazard model by Meletti *et al.* [12] was adopted in the REASSESS software tool [13] to obtain the conditional spectrum [14]. A set of 22 pairs of ground motion records [7], comprised of two horizontal components each, were taken from the PEER NGA-West 2 database [15]. The spectral acceleration, $S_a(T^*)$, at a conditioning period, T^* , was chosen as the intensity measure (IM). T^* was selected as the arithmetic mean of the fundamental periods in the two orthogonal directions of each building, as suggested in FEMA P58 [16].

The analyses carried out on the school buildings highlighted some structural deficiencies, such as excessive drifts and non-ductile collapse mechanisms. At the same time, the collapse performance characterized via the mean annual frequency of collapse (MAFC) exhibited higher values with respect to acceptable limits found in the literature [17]. Due to space limitations only a brief description of the performance assessment of the school buildings is reported in this section. However, the current performance of the school buildings can be visualized in the following sections, which are compared to the performance exhibited by the proposed retrofit strategies.



2. Retrofit of case study school buildings

The retrofit schemes for the RC building were aimed at ensuring a proper strength hierarchy in the joints and to reduce story drift concentration (i.e. soft stories). For the PC building, the strategies were focused on improving the continuity of the precast connections and on reducing the seismic demands. In the URM building, the retrofit alternatives were aimed to provide a ductile failure mode and to control the seismic actions.

In this section, some retrofit strategies are described and verified for the limit states considered [11], with the expectation of improving the overall seismic performance of the school buildings.

2.1 Retrofit alternatives for reinforced concrete building

Two retrofit alternatives were investigated for the RC school building. As illustrated in Fig. 2a, the first alternative (Alternative 1) consists of strengthening the structural elements with carbon fiber reinforced polymers (CFRP), characterized by a high tensile strength and low modulus of elasticity [18]. Alternative 1 is expected to promote a ductile failure mechanism by increasing the flexural and shear capacity in columns and joints. To design and estimate the capacity of external and corner joints, the guidelines presented by Del Vecchio *et al.* [19] were employed, whereas for internal joints the work of Akguzel and Pampanin [20] was used. The new capacity of the flexural elements strengthened with CFRP was determined through the Eurocode 8 provisions [21]. In the case of the columns, two types of CFRP products were considered: bars and wrapping sheets. Bars were aimed at increasing the column flexural capacities, whereas wrapping sheets were targeted to increase their confinement, shear capacities and deformation capacities. Continuous CFRP strips were used for beam-column joints. These strips are placed horizontally and vertically to compensate for the lack of shear capacity. This intervention foresees a proper failure sequence in the strength hierarchy of the RC column-beam joints [22].

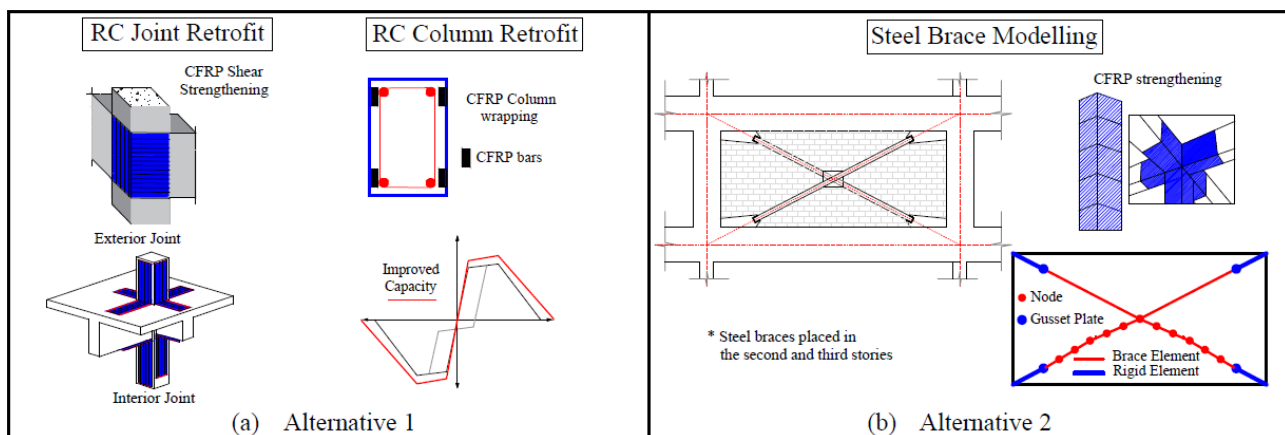


Fig. 2 - Retrofit alternatives for the RC school building where (a) Alternative 1 consists of CFRP bars, wrapping of columns and CFRP strips in joints, and (b) Alternative 2 incorporates to Alternative 1 steel braces placed in second and third stories

Alternative 2 consists of CFRP strengthening along with steel braces (Fig. 2b). The steel braces were connected at their centers to reduce the unbraced length and improve post-buckling resistance and were installed in the second and third stories of the RC school building. The additional stiffness provided by the steel braces reduces the story drifts and increases the capacity of the seismic force-resisting system, which would help prevent a potential soft-story mechanism. The design of the braces was conducted through an equivalent single-degree-of-freedom system, as described by Di Cesare and Ponzo [23]. In particular, the effect of global buckling in the steel braces was modelled using the recommendations of Lignos *et al.* [24]. An initial camber, proportional to the unbraced length, is required to induce in- and out-of-plane buckling, reproducing a realistic behavior under earthquakes loads. Following the procedure described by Uriz and



Mahin [25], it was found adequate to induce a camber of 0.75% for in-plane buckling, while 0.05% was sufficient for out-of-the plane buckling.

2.2 Retrofit alternatives for precast concrete building

For the PC school building, two retrofit alternatives were studied to solve the lack of continuity in the beam-column connections and excessive story drifts. As illustrated in Fig. 3a, Alternative 1 implements arch-shape ductile connections [26] in the upper part of the beam-column joints. As stated by Belleri *et al.* [26], the different stiffness and both in-plane and out-of-plane strengths make this connection quite effective in controlling displacements and dissipating energy. The behavior of the lower part of the joint was improved by adding some dowels that are connected with a small steel plate. In this way, the connection capacity will depend not only on friction but also on the shear capacity of the dowels [27]. Furthermore, steel braces were placed in the second story to mitigate the soft-story mechanisms. Likewise, steel beams were introduced in the transverse direction to induce a frame behavior.

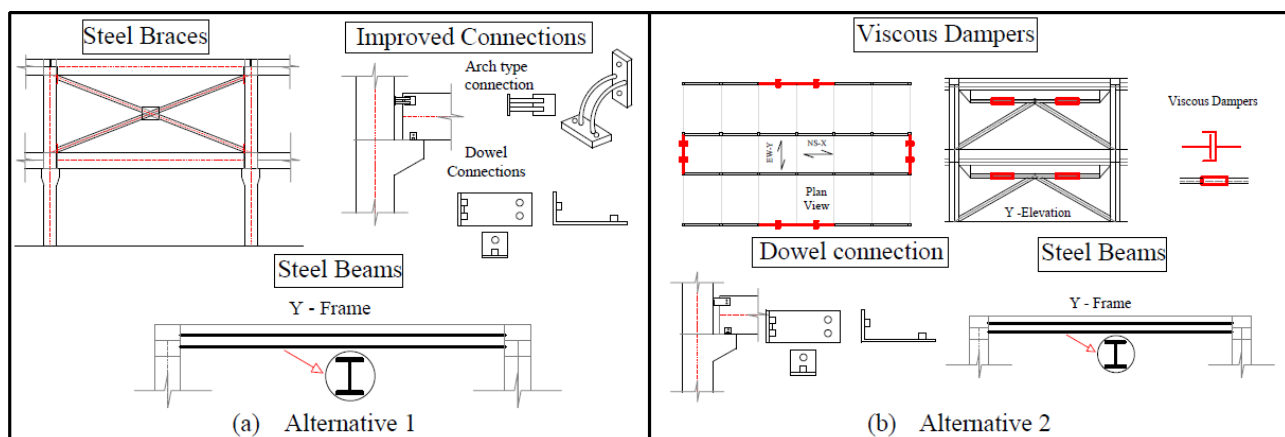


Fig. 3 - Retrofit alternatives for the PC school building where (a) Alternative 1 incorporates steel braces and improved connections in the column-beam joint, and (b) Alternative 2 includes viscous dampers and improved connections

The second retrofit alternative (Alternative 2) considers placing dowels in the upper and lower part of the joints. It also includes steel beams in the transverse direction to guarantee a frame behavior similar to Alternative 1. However, this second retrofit alternative introduces linear viscous dampers placed in different locations in the building, as shown in Fig. 3b. Assuming an inherent damping value of 5%, it was determined that a supplemental damping ratio of 15% of critical in the first mode of the building would considerably reduce the seismic demand, accounting for a total damping ratio of 20%. The amount of supplemental damping was determined by estimating the viscous damper's constant as a function of a story lateral stiffness distribution of the unbraced structure for the first two fundamental shape modes [28].

2.3 Retrofit alternatives for masonry building

Two retrofit strategies were devised to increase the structural capacity and to reduce the seismic demand in the URM school building. Alternative 1 incorporates CFRP strips on both sides of the masonry piers and spandrels, as displayed in Fig. 4a. The design of the CFRP was based on a strength criterion comparison, following the procedure described in CNR-DT 200 R1/2013 [29]. This retrofit intervention is expected to lead to a shift in failure mode, where the shear capacity is increased (dotted lines) and the flexural cracking (blue line) is now the governing failure mechanism. As a result, new drift capacities at shear and rupture for buckling failure were adopted as 0.6% and 1.2%, respectively [29, 30].

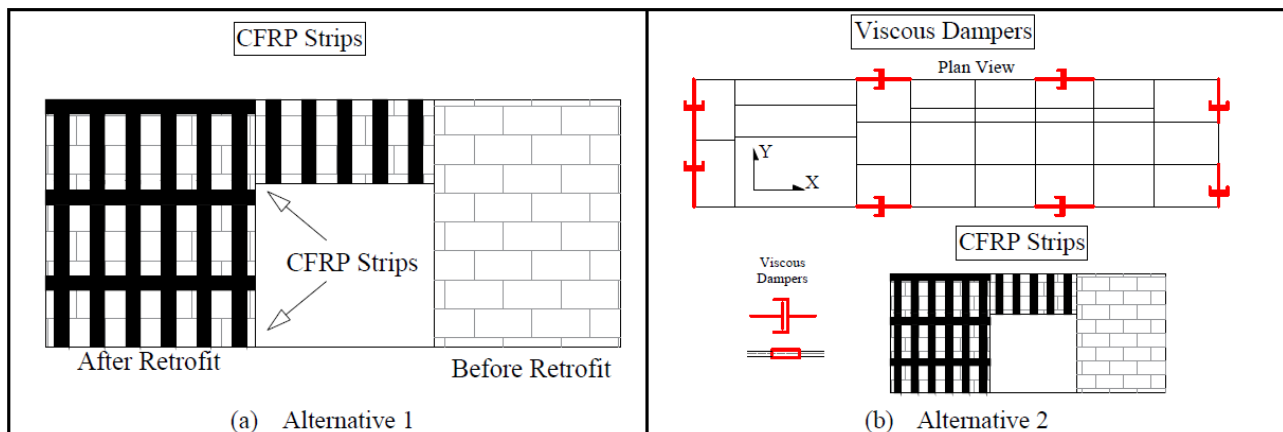


Fig. 4 - Retrofit alternatives for the URM School building where (a) consist of FRP strips and (b) introduces to alternative 1 some viscous dampers

Alternative 2 also proposes CFRP but introduces linear viscous dampers placed strategically in the school building, as illustrated in Fig. 4b. A total of 16 viscous dampers, eight per floor and four per each principal direction, were included. Assuming an inherent viscous damping ratio of 5% of critical, it was found that a supplemental damping of 35% of critical in the first mode of vibration was needed in the transverse direction (Y) whereas, in the longitudinal direction (X), only 10% supplemental damping was needed. These account for a total damping ratio of 40% and 15% damping in each principal direction, respectively. Using the option to incorporate the CFRP action on the masonry elements featured in the TreMuri software [6], the amount and properties of CFRP strips were defined and assigned in TreMuri as a special type of reinforcement. In the case of viscous dampers, their effect was included by modifying the Rayleigh damping coefficients according to their participating modes [28].

3. Assessment of retrofit alternatives

The performance assessment of the retrofitted case study school buildings was carried out both through pushover and multi-stripe analyses. On the one hand, the introduction of CFRP, defined as Alternative 1 in the RC school building, ensures a proper ductile failure sequence to the RC column-beam joints. As a result, the building's lateral strength and deformation capacity are increased in both directions. On the other hand, in Alternative 2 the steel braces increment not only the lateral stiffness but also the lateral capacity of the building, as shown in Fig. 5a. For the PC school building, both alternatives (1 and 2) implement proper connections, which remarkably modify the overall strength of the building (Fig. 5b). The steel braces of Alternative 1 significantly increase the stiffness of the system. Likewise, the steel beams in the transverse direction contribute to a frame action that greatly improves the structural behavior and lateral resistance of the building. Moreover, the supplemental viscous dampers of Alternative 2 reduce the seismic demand (i.e. story drifts and floor accelerations). Alternative 1 of the URM school building is effective in enhancing the lateral deformability and lateral resistance of the building since it changes the failure mechanism of the piers. Higher deformations are reached due to the updated drift shear and bending failure of the CFRP material defined as 0.6% and 1.2%, respectively [6, 30]. As illustrated in Fig. 5c, Alternatives 1 and 2 overlap, given that the effect of introducing viscous dampers in Alternative 2 does not affect the lateral static capacity of the building.

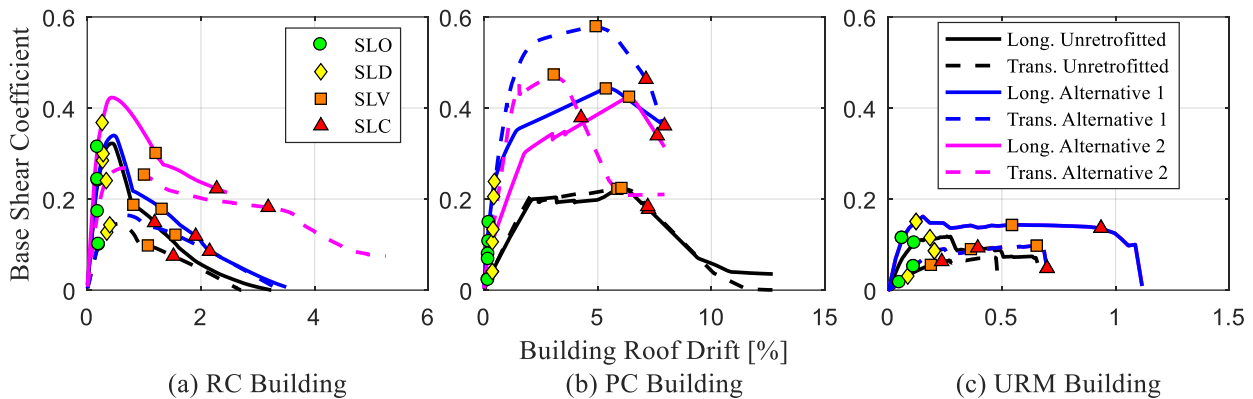


Fig. 5 - Static pushover curves for each retrofitted school building, where the base shear has been normalized by the total building weight and plotted the points at which each of the limit states are exceeded

3.1 Structural performance

The structural performances of the retrofitted alternatives were assessed through the N2 method [8, 9]. The retrofit alternatives adopted for the PC and URM buildings (Alternative 1 and 2), whose original configurations exceeded the drift limits, proved to be effective in reducing the maximum story drift for the serviceability limit states (SLO and SLD). Likewise, the RC building and its retrofit options yielded lower drifts compared to the code limits. Nevertheless, for the ultimate limit states (SLV and SLC), only Alternative 2 of the RC school building, worked quite well in reducing drifts. Alternative 2 avoids soft/weak story mechanisms. For the PC building, both alternatives significantly reduce the story drifts. Indeed, Alternative 2 achieved a greater reduction and uniform story drift distribution as a result of the supplemental damping provided by the viscous dampers. Finally, for the URM building, the ultimate limit states were only satisfied when adopting Alternative 2. Although Alternative 1 in the URM school building achieved a larger building strength and deformation capacity, it was not able to satisfy the seismic demand for the ultimate limit state (SLC) in the transverse direction.

The results of the multi-stripe analyses showed that the adoption of the retrofit alternatives also modifies the peak story drift (PSD) and peak floor acceleration (PFA) profiles. The strategies of implementing steel braces and better connections decrease the PSD but amplify the PFA. However, the alternatives based on viscous dampers achieve a reduction on both demand parameters. More importantly, as illustrated in Fig. 6, all retrofit interventions considerably improve the collapse fragility functions of the school buildings, meaning that these buildings are less prone to collapse as their fragility curves shifted to the right.

The collapse margin ratio (CMR), defined as the ratio between the median collapse intensity and the intensity at SLC, can be used as an indicator of the collapse improvement. Table 1 reports the median collapse intensity (θ) as well as the total dispersion (β_T) and CMR for each configuration. The factor β_T accounts for two types of dispersion: record-to-record variability and modelling uncertainty. Both retrofitted alternatives of the RC school building present a higher CMR compared to the original configuration (unretrofitted). For the PC building, the CMR for the two retrofitted alternatives demonstrate that they improve the collapse vulnerability of the building, with Alternative 2 exhibiting a CMR slightly larger than that of Alternative 1. Finally, for the URM school building, both retrofit alternatives considerably improve the collapse performance. However, Alternative 1 is not sufficient to provide a CMR larger than unity, whilst Alternative 2 achieves this goal, thereby ensuring a greater reduction in collapse vulnerability.

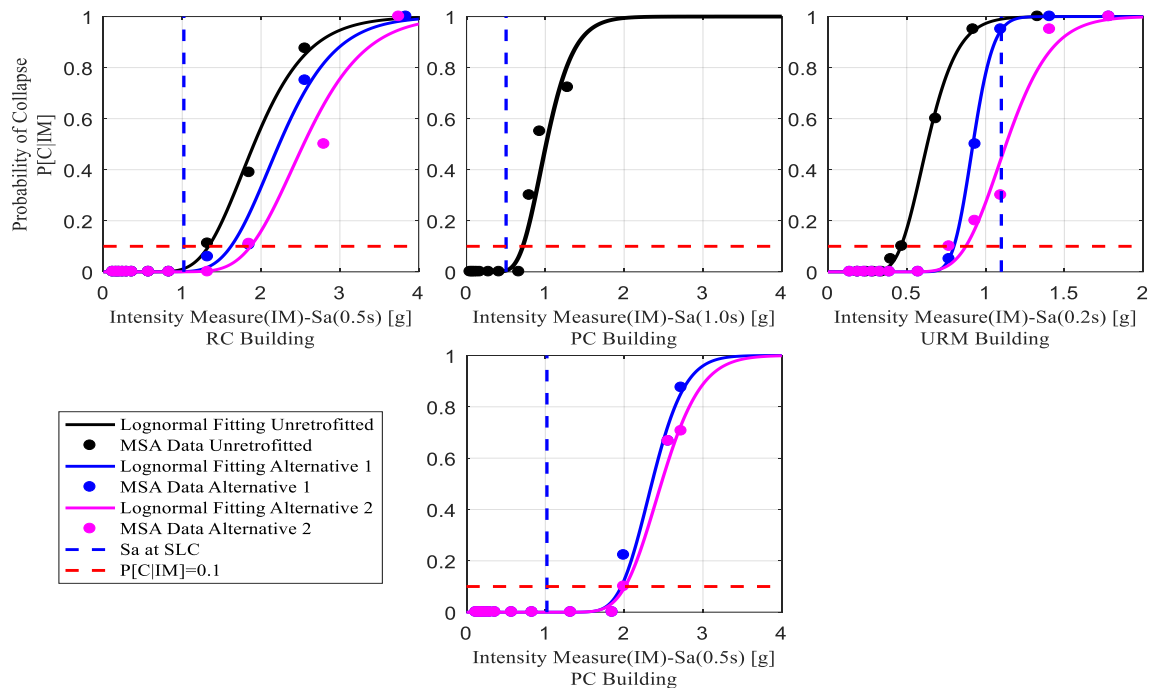


Fig. 6 - Collapse fragility functions for each retrofitted school building (Note: the differing conditioning periods of the PC retrofit alternatives mean that no direct comparison can be made).

The mean annual frequency of collapse (MAFC) for the three case study school buildings is reported in Fig. 7. The MAFC is obtained by integrating the collapse fragility function with the site hazard curve over a range of intensities. Both retrofit alternatives of the RC school building reduce the risk of collapse, placing the retrofitted building within the acceptable limits suggested by Dolšek *et al.* [17]. Although Alternative 1 of the PC school building achieves a reduction of 38% in MAFC, with respect to the unretrofitted configuration, this value is still slightly above the recommended MAFCs. Only Alternative 2 is achieving a MAFC value within the suggested limits. Even though both retrofit alternatives of the URM school building reach a reduction of 67% and 76% in MAFC, respectively, in comparison to the original building, the suggested limits are still largely exceeded.

Table 1 - Median collapse intensities, θ , and dispersion due to record-to-record variability, β_T , for each retrofitted school building

School building	Retrofit Alternative	Median collapse intensity, θ [g]	Total dispersion, β_T	Sa at SLC [g]	Collapse margin ratio (CMR)
RC	Unretrofitted	1.91	0.32	1.02	1.87
	Alternative 1	2.23	0.29		2.19
	Alternative 2	2.48	0.28		2.43
PC	Unretrofitted	1.01	0.44	1.02	2.01
	Alternative 1	2.35	0.38		2.30
	Alternative 2	2.47	0.38		2.42
URM	Unretrofitted	0.63	0.31	1.10	0.57
	Alternative 1	0.92	0.23		0.84
	Alternative 2	1.13	0.28		1.03



3.2 Loss estimation

Table 2 lists the expected annual loss (EAL) values of each building model. The EAL reduction achieved by the retrofit strategies for the RC school building is not substantial. On the one hand, the EAL (0.25%) of Alternative 1 is very close to the EAL (0.27%) of the unretrofitted building since Alternative 1 resulted in similar PFAs and PSDs when compared to the original model. Alternative 2 reduces the PSD but increases the PFA, which causes an offset between the expected losses of drift- and acceleration-sensitive non-structural elements. By contrast, Alternative 2 of the PC and URM school buildings results in a remarkable reduction of the EAL. This is the result of lower PFAs and PSDs attained by the viscous dampers. As shown in Table 2, the EAL of each model is based on the total replacement cost of each building typology. These costs were estimated using a cost per floor area approach, rather than an individual component-based cost summation approach, thereby remaining unchanged for each alternative.

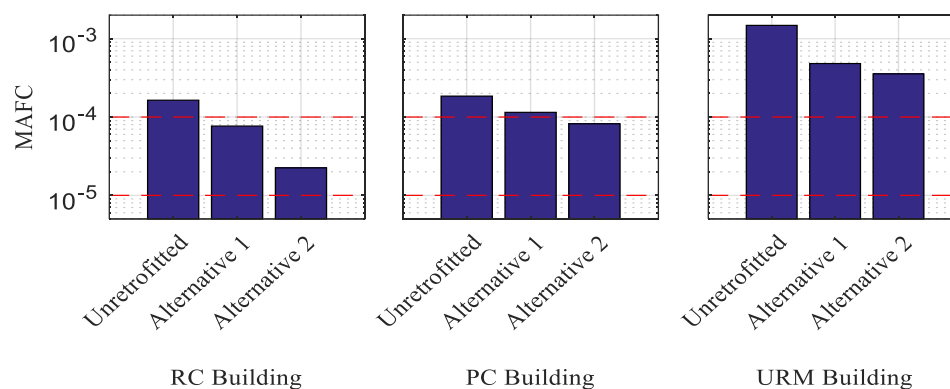


Fig. 7 - Mean annual frequency of collapse (MAFC) for the original (unretrofitted) and retrofitted school buildings

Table 2 - Expected annual loss ratios and total replacement cost for each original (unretrofitted) and retrofitted school building

School buildings	Retrofit Alternatives	Expected annual loss [%]	Replacement Cost [€]
RC	Unretrofitted	0.27	3,929,937
	Alternative 1	0.25	
	Alternative 2	0.26	
PC	Unretrofitted	0.27	4,212,616
	Alternative 1	0.25	
	Alternative 2	0.09	
URM	Unretrofitted	0.43	2,075,892
	Alternative 1	0.22	
	Alternative 2	0.19	

4. Application of Sismabonus to national scale

The Sismabonus approach [31] provides a straightforward risk classification system for existing buildings across the Italian territory. The classification framework is based on two parameters, the life safety index (IS-V) and the EAL. According to the building's performance, each parameter receives a ranking class, where the most critical parameter defines the overall risk classification of a building. The parameter IS-V is computed as the ratio between the capacity and demand expressed in terms of peak ground accelerations



(PGAs) at the life-safety limit state (SLV). Whereas, the EAL is estimated through the mean annual frequency of exceedance (MAFE) of the PGA for each limit state. This procedure is comprehensively illustrated in O'Reilly *et al.* [7]. The Sismabonus approach can also be applied at a national scale in order to estimate the seismic risk of the Italian school building typologies.

In this study, the Sismabonus methodology was applied to the case study buildings and was extended to the national scale. It is worth noting that the methodology, and its extensions to the national scale, relies on many simplifications and assumptions, so any conclusions drawn should be treated as indicative rather than accurate estimation of the risk at which the school buildings are prone. However, the findings can provide a good idea of the risk of the studied building typologies and the suitability of their retrofit strategies on reducing risk. Therefore, the risk classification was carried out as described above for a single building, but considering all hazard curves in Italy (i.e. diverse PGAs), available from [32]. This same procedure has been implemented by Perrone *et al.* [33], but in this paper the approach is also applied to the different retrofit configurations.

The risk classification of the RC school buildings in Italy, illustrated in Fig. 8, demonstrates the effectiveness of the two proposed retrofit strategies for mitigating the risk. The life-safety index determined for the unretrofitted RC school buildings is quite satisfactory in most of the Italian territory (class A+ and A), and acceptable (class B and C) for the regions of Umbria, Abruzzo, Campania, Basilicata, Calabria and Sicily. However, the risk classification of the Italian peninsula is governed by the EAL parameter (e.g. class E to G), resulting in the overall risk classification displayed in Fig. 8a. Only some northern regions of Italy (i.e. Lombardy and Trentino) as well as the south of Puglia accounts for the lowest EAL rankings (blue zones). Both retrofit schemes improve the life-safety index for this building typology, upgrading it to class A+ along all the Italian peninsula. Yet, just alternative 2 (Fig. 8c) achieved a better improvement in terms of EAL, upgrading the seismic risk of RC school buildings into the first classes and placing the most critical regions (e.g. Umbria, Abruzzo, Campania, Basilicata, Calabria and Sicily) in a low-risk zone.

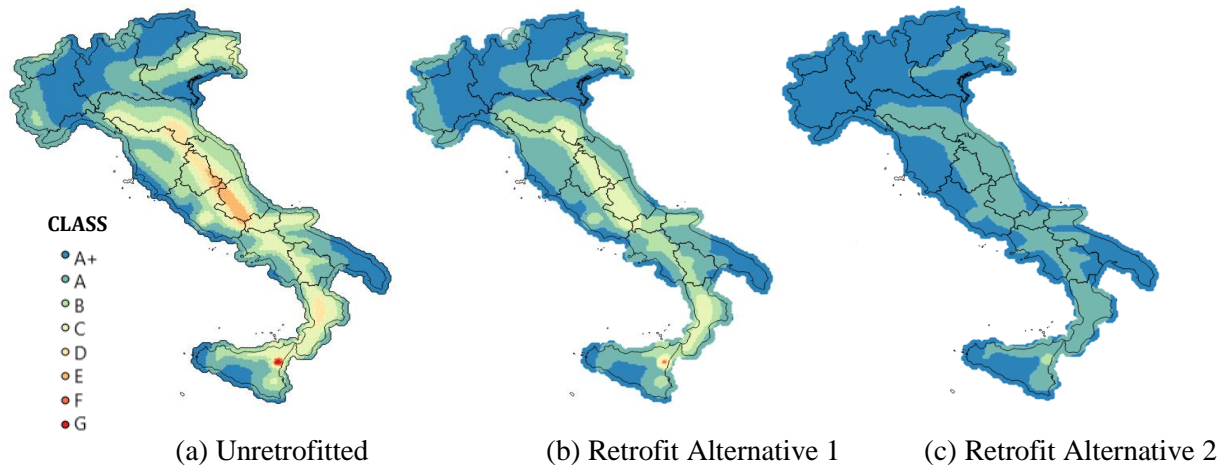


Fig. 8 - Relative comparison of overall risk classification for original (unretrofitted) and retrofitted RC school buildings located in Italy

Moreover, the risk classification of the PC school buildings on the Italian peninsula is displayed in Fig. 9a. For this typology, the controlling parameter is the EAL, with higher intensities (i.e. red zones) in the regions of Umbria, Abruzzo, Campania, Basilicata, Calabria and Sicily. Unlike the EAL, the life-safety index is not a critical indicator since all the unretrofitted PC school buildings on the Italian peninsula are categorized as class A+. The retrofit alternatives studied for this building typology exhibit an improvement in terms of EAL, decreasing this parameter for central Italy. Alternative 1 (Fig. 9b) provides a substantial reduction of EAL and IS-V in the Italian peninsula, upgrading the overall risk of this building typology to the first classes.



The URM School buildings are the most vulnerable school buildings on the Italian peninsula, as illustrated in Fig. 10a. The risk classification for this typology is controlled by the life-safety index. The retrofit Alternative 1 (Fig.10b) upgrades the IS-V class of the URM school buildings into a safe zone (first classes) but the EAL is barely changed. Only Alternative 2 (Fig. 10c) achieved a significant improvement in both classification parameters and thereby reaching a better risk class. Indeed, based on the class ranking, retrofitted URM school buildings located in regions such as Emilia Romagna, Umbria, Abruzzo and Catania can be considered at low seismic risk, while retrofitted URM school buildings in other locations are recognized as safer.

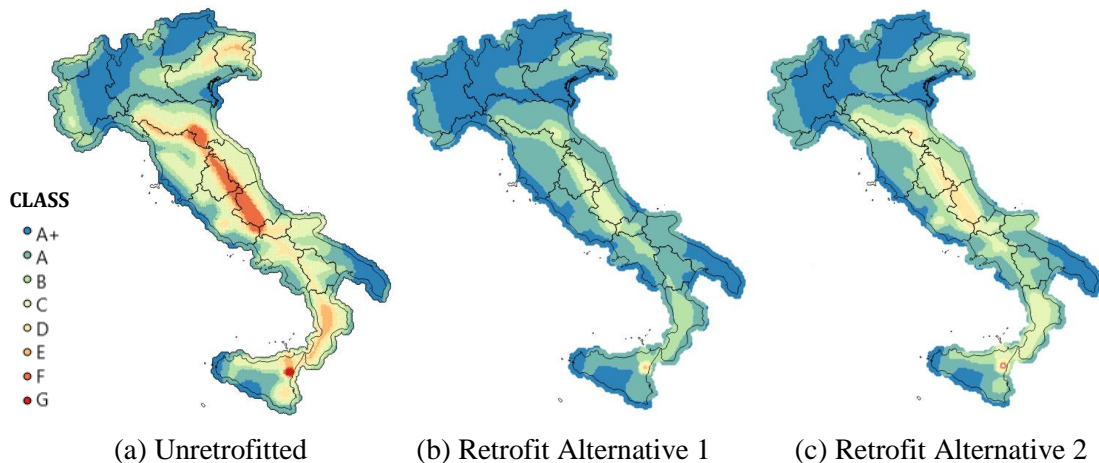


Fig. 9 - Relative comparison of overall risk classification for original (unretrofitted) and retrofitted PC school buildings located in Italy

The application of the Sismabonus methodology on the Italian peninsula pointed out that school buildings of similar typology are potentially at high risk, especially for PC and URM school buildings located in the regions of Umbria, Abruzzo, Campania, Basilicata, Calabria and Sicily (Catania). A lower, but always considerable, seismic risk has been observed for RC school buildings within the Italian territory. The results of this regional-scale application are considered practical to governmental decision-makers who would need to decide and justify the distribution of limited financial resources in a risk agenda that aim to reduce the overall seismic risk of the Italian school building stock.

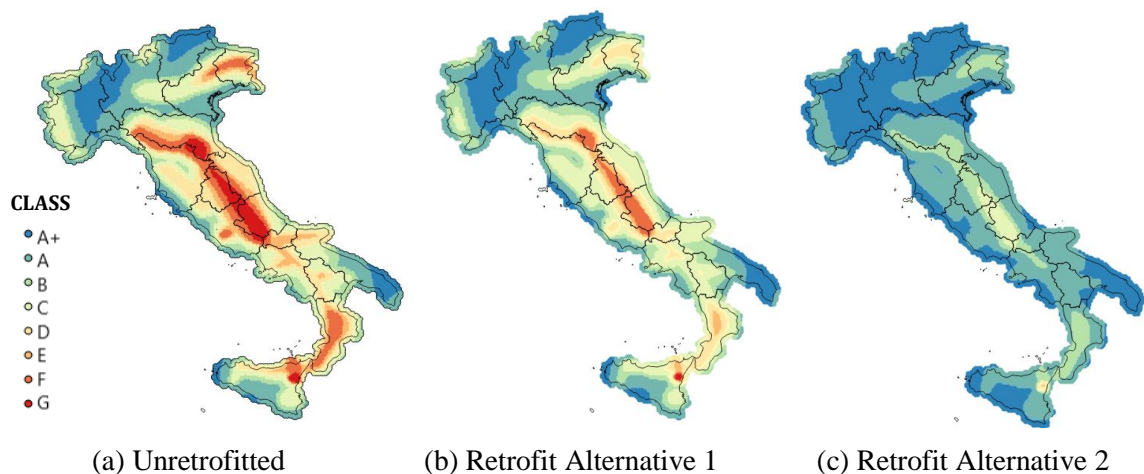


Fig. 10 - Relative comparison of overall risk classification for original (unretrofitted) and retrofitted URM school buildings located in Italy



5. Conclusions

This paper discussed different retrofit strategies aimed at improving the overall seismic response of school buildings in Italy. Three case study school buildings were selected and comprised reinforced concrete (RC), precast concrete (PC) and unreinforced masonry (URM) structural typologies. This study highlights the seismic vulnerability of these school buildings, both in terms of economic losses and inadequate structural capacity. As expected, the URM school building is the most vulnerable building. Even though the PC and RC school buildings are less vulnerable, they still present structural deficiencies, leading to non-ductile failure mechanisms. For each building configuration, two retrofit alternatives were proposed and assessed. Through the implementation of carbon fiber reinforced polymers, proper strength hierarchy in beam-column joints was achieved for the RC school building. Likewise, flexural cracking was ensured as the controlling failure mechanism in the piers of the URM school building. Better connection continuity (arch-type and dowel connections) was provided between precast elements in the PC school building. Similarly, the introduction of steel braces increased the lateral stiffness and strength capacity in the PC and RC school buildings, thereby mitigating the formation of soft/weak story mechanisms. Additionally, viscous dampers proved to be quite effective in reducing the seismic demands in terms of story drifts and floor accelerations. The strategies improved the structural capacity of the buildings, reducing their collapse vulnerability as well as the expected annual losses and mean annual frequency of collapse. However, some of the retrofit strategies were not able to meet code requirement and to place the mean annual frequency of collapse within the suggested limits. Moreover, the application of the Sismabonus guidelines to a national scale gave a good representation of the national seismic risk of these school buildings and how the retrofit strategies mitigate this problem. In fact, the retrofit interventions attenuated the risk along all the Italian peninsula. These results, although affected by many assumptions and simplifications, provided a clear view of the regions where higher investments are needed to reduce the seismic risk of school buildings.

6. Acknowledgements

This paper has been developed within the framework of the project “Dipartimenti di Eccellenza”, funded by the Italian Ministry of University and Research at the University School for Advanced Studies IUSS Pavia. The authors acknowledge also the support of the ReLUIS consortium within the 2019-2021 research grant.

7. References

- [1] Borzi B, Ceresa P, Faravelli M, Fiorini E, Onida M (2011): Definition of a prioritization procedure for structural retrofitting of Italian school buildings. *COMPADYN 2011-3rd ECOMAS Themat Conf Comput Methods Struct Dyn Earthq Eng*, Corfu, Greece.
- [2] Perrone D, O'Reilly GJ, Monteiro R, Filiatrault A (2019): Assessing seismic risk in typical Italian school buildings: from in-situ survey to loss estimation. *International Journal of Disaster Risk Reduction*, <https://doi.org/10.1016/j.ijdrr.2019.101448>.
- [3] Buratti N, Minghini F, Ongaretto E, Savoia M, Tullini N (2017): Empirical seismic fragility for the precast RC industrial buildings damaged by the 2012 Emilia (Italy) earthquakes. *Earthquake Engineering & Structural Dynamics*. **46** (14), 2317-2335, <https://doi.org/10.1002/eqe.2906>.
- [4] Penna A, Morandi P, Rota M, Manzini CF, Da Porto F, Magenes G (2014): Performance of masonry buildings during the Emilia 2012 earthquake. *Bull Earthq Eng*. **12**, 2255–73, <http://dx.doi.org/10.1007/s10518-013-9496-6>.
- [5] McKenna F, Scott MH, Fenves GL (2010): Nonlinear finite-element analysis software architecture using object composition. *J Comput Civ Eng*. **24**, 95–107, [http://dx.doi.org/10.1061/\(ASCE\)CP.1943-5487.0000002](http://dx.doi.org/10.1061/(ASCE)CP.1943-5487.0000002).
- [6] Lagomarsino S, Penna A, Galasco A, Cattari S (2013): TREMURI program: an equivalent frame model for the nonlinear seismic analysis of masonry buildings. *Eng Struct*. **56**, 1787–99, <http://dx.doi.org/10.1016/j.engstruct.2013.08.002>.
- [7] O'Reilly G, Perrone D, Fox M, Monteiro R, Filiatrault A (2018): Seismic assessment and loss estimation of existing school buildings in Italy. *Eng Strct*. **168**, 142-162, <https://doi.org/10.1016/j.engstruct.2018.04.056>.



- [8] Fajfar P (2000): A nonlinear analysis method for performance based seismic design. *Earthquake Spectra*, **16** (3), 573-592.
- [9] Dolšek M, Fajfar P (2005): Simplified non-linear seismic analysis of infilled reinforced concrete frames. *Earthquake Engng Struct. Dyn.* **34** (1), 49-66, <https://doi.org/10.1002/eqe.411>.
- [10] Dolšek M, Fajfar P (2004): Inelastic spectra for infilled reinforced concrete frames. *Earthquake Engng Struct. Dyn.* **33** (15), 1395-1416, <https://doi.org/10.1002/eqe.410>.
- [11] NTC (2018): Norme Tecniche Per Le Costruzioni. Rome, Italy.
- [12] Meletti C, Galadini F, Valensise G, Stucchi M, Basili R, Barba S, Vannucci G, Boschi E (2008): A seismic source zone model for the seismic hazard assessment of the Italian territory. *Tectonoph.* **450**, 85-108, <https://doi.org/10.1016/j.tecto.2008.01.003>.
- [13] Iervolino I, Chioccarelli E, Cito P (2015): REASSESS V1.0: A computationally efficient software for probabilistic seismic hazard analysis. In: *COMPDYN 2015–5th ECCOMAS themat conf comput methods struct dyn earthq Eng*, Crete Island, Greece.
- [14] Baker JW (2011): Conditional mean spectrum: tool for ground motion selection. *Journal of Structural Engineering*, **137** (3), 322-331, [http://dx.doi.org/10.1061/\(ASCE\)ST.1943-541X.0000215](http://dx.doi.org/10.1061/(ASCE)ST.1943-541X.0000215).
- [15] Ancheta TD, Darragh RB, Stewart JP, Seyhan E, Silva WJ, Chiou BSJ (2013): PEER NGA-West2 Database. PEER Rep 2013/03.
- [16] FEMA P58-1 (2012): Seismic performance assessment of buildings: volume 1 - methodology (P-58-1). vol. 1. Washington, DC.
- [17] Dolšek M, Lazar Sinković N, Žižmond J (2017): IM-based and EDP-based decision models for the verification of the seismic collapse safety of buildings. *Earthq Eng Struct Dyn.* **46**, 2665–82, <http://dx.doi.org/10.1002/eqe.2923>.
- [18] Mugahed Y, Rayed A, Raizal S, Hisham A, Hunge C (2018): Properties and applications of FRP in strengthening RC structures: A review. *Structures*. **16**, 208-238, <https://doi.org/10.1016/j.istruc.2018.09.008>.
- [19] Del Vecchio C, Di Ludovico M, Prota A, Manfredi G (2015): Analytical model and design approach for FRP strengthening of non-conforming RC corner beam-column joints. *Engineering Structures*. **87**, 8-20, <https://doi.org/10.1016/j.engstruct.2015.01.013>.
- [20] Akguzel U, Pampanin S (2012): Assessment and design procedure for the seismic retrofit of reinforced concrete beam-column joints using FRP composite materials. *ASCE, J. Compos. Constr.* **16** (1), 21-34.
- [21] EN 1998-3 (2005): Eurocode 8: Design of structures for earthquake resistance – Part 3: Assessment and retrofit of buildings. Brussels, Belgium.
- [22] Tasligedik S, Akguzel U, Kam W, Pampanin S (2016): Strength hierarchy at reinforced concrete beam-column joints and global capacity. *Journal of Earthquake Engineering*. 1-34.
- [23] Di Cesare A, Ponzio F (2017): Seismic retrofit of reinforced concrete frame buildings with hysteretic bracing systems: design procedure and behavior factor. *Shock and Vibration*, <https://doi.org/10.1155/2017/2639361>.
- [24] Lignos DG, Karamanci E, Martin G (2012): A Steel database for modelling post-buckling behavior and fracture of concentrically braced frames under earthquakes. *15th World Conference on Earthquake Engineering*, Lisbon, Portugal.
- [25] Uriz, P, Mahin, SA (2008): Toward earthquake-resistant design of concentrically braced steel-frame structures. *PEER Report 2008/08*, Berkeley, California.
- [26] Belleri A, Torquati M, Riva P (2013): Seismic performance of ductile connections between precast beams and roof elements. *Magazine of Concrete Research*. **66** (11), 553-562, <https://doi.org/10.1680/macr.13.00092>.
- [27] Fib (2008): Structural connections for precast concrete building, guide to good practice. *Bulletin 43*.
- [28] Constantinou MC, Soong TT, Dargush GF (1998): Passive energy dissipation systems for structural design and retrofit, *Monograph No1. Multidisciplinary Center for Earthquake Engineering Research*. University of Buffalo, State University of New York, Buffalo, NY.
- [29] CNR-DT 200 R1/2013 (2013): Consiglio nazionale delle ricerche. Istruzioni per la progettazione, l'esecuzione ed il controllo di interventi di consolidamento statico mediante l'utilizzo di compositi fibrorinforzati.
- [30] Morandi P, Albanesi L, Graziotti F, Li Piani T, Penna A, Magenes G (2018): Development of a dataset on the in-plane experimental response of URM piers with bricks and blocks. *Construction and Building Materials*. **190**, 593-611, <https://doi.org/10.1016/j.conbuildmat.2018.09.070>.
- [31] Cosenza E, Del Vecchio C, Di Ludovico M, Dolce M, Moroni C, Prota A, Renzi E (2018): The Italian guidelines for seismic risk classification of constructions: technical principles and validation. *Bulletin of Earthquake Engineering*. **16**, 5095-5935, <https://doi.org/10.1007/s10518-018-0431-8>.
- [32] Stucchi M, Meletti C, Montaldo V, Crowley H, Clavi GM, Boschi E (2011): Seismic hazard assessment (2003-2009) for the Italian Building Code. *Bulletin of the Seismological Society of America*. **101** (4), 1885-1991.
- [33] Perrone D, O'Reilly G, Monteiro R, Filiatrault A (2019): Assessing seismic risk in typical Italian school buildings: from in-situ survey to loss estimation. *International Journal of Disaster Risk Reduction (IJDRR)*.